

IN SITU CHARACTERIZATION OF GRINDING WHEEL SURFACE

Akira HOSOKAWA, Kunio SAKUMA and Takashi UEDA
 Department of Mechanical Systems Engineering, Kanazawa University
 2-40-20 Kodatsuno, Kanazawa 920-8667, Japan

1. INTRODUCTION

In grinding operation, machining accuracy and surface finish depend directly on the grinding wheel topography: shape and distribution of cutting grains on the wheel surface. Therefore, several techniques have been developed concerning the measurement of wheel topography such as profilometry, dynamometry, microscopy and others [1]. In-process measurement is actually desirable because the condition of a wheel surface is likely to change during grinding.

In this study, an in-process characterization of the wheel surface is proposed, where the grinding sound and/or vibration are analyzed by a neural network technique. The in-cycle measurements of the static wheel topography are also developed, in which a stylus profilometer and a digital image scope are equipped on the grinding machine [2, 3].

2. EXPERIMENTAL PROCEDURE

Parameters for characterizing grinding wheel surface are classified into two categories: 'static' and 'dynamic' parameters. In the static evaluation, the wheel surface is directly measured by means of the stylus method or the microscopic observation. In the dynamic measurement, on the other hand, the wheel condition is evaluated by analyzing the grinding sound and/or vibration, which are generated by the wheel-work interaction in the grinding zone. In this method, however, it is difficult to quantify the geometrical or morphological characteristics of the wheel surface from these signals in the present stage. Hence several conditions of the wheel surface—standard or reference condition—are formed by dressing and the grinding sound/vibration generated by these wheels are regarded as the standard signals. Then the sound/vibration during grinding are discriminated by a neural network technique.

2.1 Conventional Vitrified-Bond Alumina Wheel

2.1.1 Formation of wheel surface

In order to form a reference wheel surface, the wheel is dressed in some dressing conditions as shown in Table 1. The variations of tangential grinding force F_t and three-dimensional arithmetic average roughness

Condition No.	Dressing depth a_d μm	Dressing feed s_d $\mu\text{m}/\text{rev}$
(1)	5	20
(2)	20	20
(3)	5	100
(4)	20	100
(5)	5	200
(6)	20	200

Dresser : Single-point diamond dresser

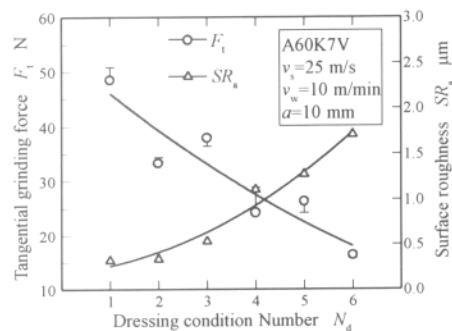


Fig.1 Variations of tangential grinding force and surface roughness with dressing conditions

SR_a with dressing conditions are shown in Fig.1. It is found from the figure that six different surface are generally formed although clear distinction does not appear between the condition-(2) and (3); and the condition-(4) and (5).

2.1.2 Experimental setup and conditions

Figure 2 shows the experimental arrangement. The plunge grinding of carbon steel at a constant depth of cut is carried out with six different wheel conditions presented in Table 1. The grinding sound, vibration and grinding forces are measured by the noise level meter, accelerometer and piezoelectric dynamometer, respectively. The acceleration pickups are fixed on the high-stiffness mount base as shown in Fig.2 in order to avoid the vibration effect of the dynamometer. Three one-pass plunge grinding tests are done in each wheel condition. The experimental conditions are summarized in Table 2.

2.2 Superabrasive Resinoid-Bonded Diamond Wheel

2.2.1 Formation of wheel surface

Because of the non-porous type grinding wheel, the resinoid-bonded diamond wheel is firstly trued by the metal-bonded diamond block truer and then the bond material is removed by dressing with WA-stick so as to make appropriate chip pocket. Here, four reference surface conditions are formed having the different depth of chip pocket. In this case, unlike the alumina wheel, there is little difference of cutting edge geometry in each wheel surface.

2.2.2 Characterization of wheel topography by stylus method and optical microscopy

A profile trace along the circumference of the wheel is measured by a stylus coupled to a displacement transducer mounted on the grinding machine, and the average depth of chip pocket h_p is calculated from the digitized profile data [2]. Figure 3 shows the definition of h_p and examples of wheel profiles of four reference conditions. It is found that the depth of chip pocket changes in four steps within the range of approximately 9~25 μm at about 5 μm intervals. The morphology of abrasive grains is observed by the digital image microscope and the distribution of cutting edges is calculated by means of an image processing method [3].

The grinding experiments are carried out in a similar way to that with the alumina wheel as described in §2.1.2. The truing and dressing conditions are listed in Table 3.

3. EVALUATION OF GRINDING WHEEL SURFACE BY MEANS OF NEURAL NETWORK TECHNIQUE

The frequency spectrum of grinding sound emitted from the standard wheel surface are discriminated by the neural network learning algorithm. The network program is constructed on the MATLAB® software. The

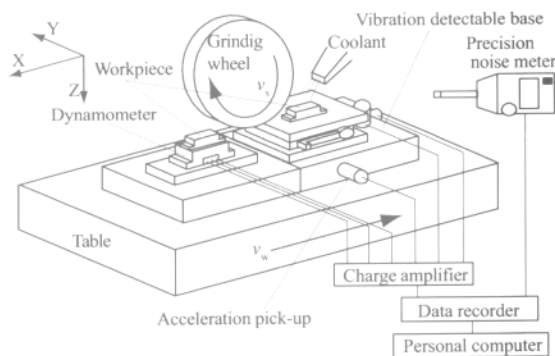


Fig.2 Experimental setup

Table 2 Experimental conditions

Grinding wheel	A60K7V	SDC140N75B
Workpiece	S55C(AISI 1055)	HIP-Si ₃ N ₄
Wheel speed v_s m/s	25	25
Work speed v_w m/min	10	10
Depth of cut a μm	10	2
Grinding fluid	Water-based solution type	

Table 3 Truing and dressing conditions of SDC140N75B-wheel

Truing	Dressing
Truer : SD100Q100M-block	Dresser : WA180H7V-stick
Truing depth a_t 2 μm	Dressing depth a_d 50 μm
Table speed v_w 10 m/min	Table speed v_w 10 m/min
Truing feed s_t 50 $\mu\text{m}/\text{rev}$	

parameters of the neural the network used are listed in **Table 4**. The input signal is described $[501 \times N]$ matrix which consists of N column vector with 501 elements of SPL (Sound Pressure Level) values within a range of 0 to 10 kHz at 20 Hz intervals. Here N is the number of reference conditions ($N=6$: alumina wheel, $N=4$: diamond wheel). The network produces $[N \times N]$ diagonal matrix. The grinding sound discrimination is judged by the position of the maximum value on the i -th row against the j -th column in the output matrix. In this experiment, the multiple layer networks are constructed and the learning algorithm is error-back-propagation (EBP) method.

It is necessary to determine the optimal learning rate and number of cells in hidden layer by learning experiments. In this study, the number of epochs required for network convergence is measured under various network configuration in which the number of cells in hidden layer and learning rate are changed in the range of 100~500 (alumina wheel) / 50~400 (diamond wheel) and 0.001~0.0005 (at 0.0003 intervals), respectively. Learning stops when either the number of epochs have attained a maximum value of 3000 or the network sum-squared error has dropped below the error goal of 0.1.

4. EXPERIMENTAL RESULTS

4.1 Conventional Vitrified-Bond Alumina Wheel

Figure 4 shows the typical frequency spectrum of the grinding sound for six reference conditions of the wheel surface. All spectrum curves have the similar pattern showing the almost flat response in the whole range although small peak appears at 2~3kHz. According to this figure, it is obvious that we can not distinguish these sounds aurally.

Figure 5 represents the learning result of the neural network as a mesh plot when the frequency spectrums of the grinding sound are discriminated. As the diagram indicates, learning begins to converge when the

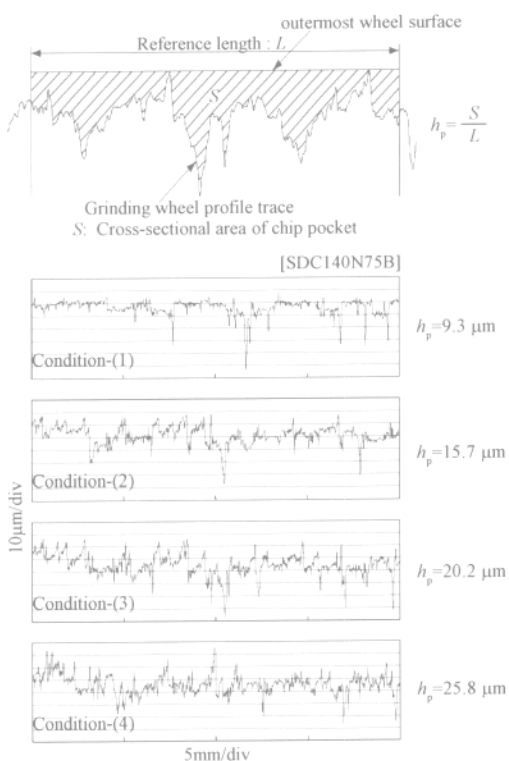


Fig.3 Definition of depth of chip pocket h_p and typical circumferential profiles of dressed wheel surface

Table 4 Parameters of neural network configuration

Structure	Multiple layer network
Hidden layer	1
Cell	Static analog model
Learning algorithm	EBP:Error Back Propagation
Transfer function	Log-sigmoid
Number of cells in input layer	501
Number of cells in hidden layer	100~500
Number of cells in output layer	6 or 4

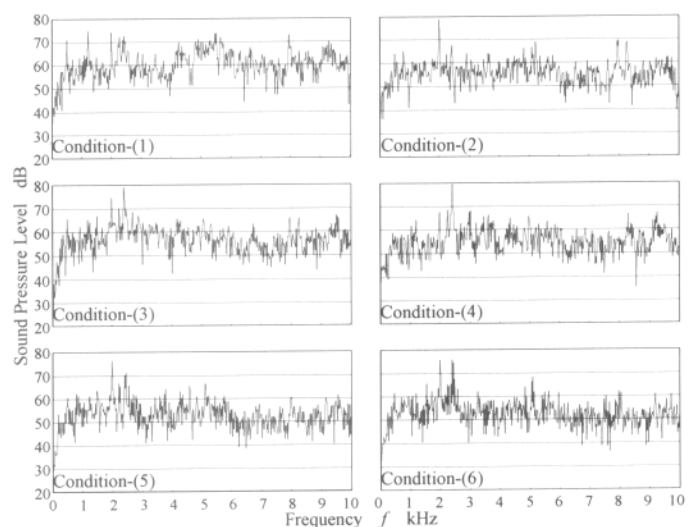


Fig.4 Frequency spectrum of grinding sound for six kinds of grinding wheel conditions

number of cells in hidden layer is more than about 100 and the number of epoch decreases as the number of cells increases. In addition, the larger a learning rate the less time a network needs to be trained. However, if the learning rate is too large learning becomes unstable, which is the general tendency of a neural network [4]. On the whole, the grinding sound can be identified under the optimum network configuration in such that the learning rate is set in the range of 0.002~0.0035 and the number of cells in hidden layer is not less than 300.

The output matrix for the discrimination of grinding sound is presented in Fig.6. In this matrix, the largest values are positioned diagonally, which means that the wheel surface is successfully recognized. From the above results, it can be said that the condition of the wheel surface is discriminated by the neural network technique in spite of acoustically indistinctive situation. After re-dressing, however, the network classifies into three categories: condition-(1), (2)~(5) and (6). One of the reasons for this result is that the equivalent wheel surface is not created by dressing. There is room for further investigation on the learning algorithms of the network.

4.2 Superabrasive Resinoid-Bonded Diamond Wheel

In the case of the resinoid-bonded diamond wheel, the number of cells in output layer is four because four kinds of standard wheel conditions are formed. The learning result of the neural network is shown in Fig.7, in which stable learning are obtained as in the case of the alumina wheel.

5. CONCLUSIONS

The neural network technique is effective to recognize the difference of the grinding wheel surface for both conventional alumina wheel and superabrasive diamond wheel by analyzing the grinding sound insofar as the wheel topography is relatively widely changed by dressing procedure. This method is found to be useful for in-situ characterization of the wheel surface.

REFERENCES

- [1] Verkerk, J., "Final Report Concerning CIRP Cooperative Work on the Characterization of Grinding Wheel Topography," Annals of the CIRP, Vol.26, No.2, 1977, pp.385-395.
- [2] Nakazono, H., Yasui, H., Kurusu, M. and Hosokawa, A., "Studies on Dressing of the Resin-Bond CBN Grinding Wheel (1st Report)," Bull. JSPE, Vol.24, No.1, 1990, pp.51-56.
- [3] Hosokawa, A., Yasui, H. and Nagae, Y., "Characterization of Grinding Wheel Surface by Means of Image processing," Proc. CESA'96 IMACS Multiconference, 1996, pp.428-32.
- [4] Uesaka, Y., "Fundamental Mathematics for Neurocomputing," Kindaikagaku-sha, 1997.

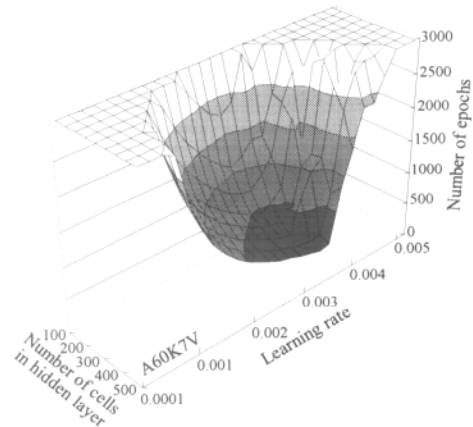


Fig.5 Learning result of grinding sound discrimination

Cond.-(1)	Cond.-(2)	Cond.-(3)	Cond.-(4)	Cond.-(5)	Cond.-(6)
0.6364	0.0577	0.0834	0.0482	0.0164	0.0287
0.1063	0.2657	0.0533	0.0605	0.1109	0.0591
0.0557	0.1949	0.4043	0.0432	0.0674	0.0993
0.0957	0.0434	0.0858	0.4275	0.0751	0.0533
0.0186	0.0615	0.0344	0.1550	0.5972	0.0513
0.0286	0.0411	0.0765	0.0355	0.0770	0.7497

Fig.6 Output matrix of grinding sound discrimination

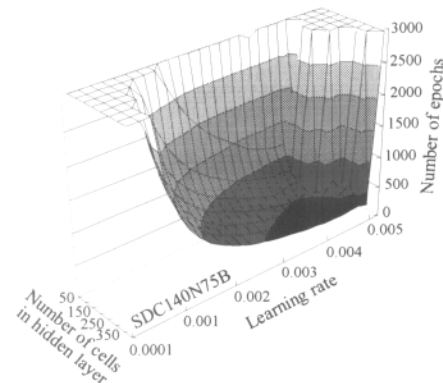


Fig.7 Learning result of neural network for SDC140N75B-wheel